

TWO DIMENSIONAL ARRAY OF ANTENNA-COUPLED MICROBOLOMETERS

F. J. González,¹ M. A. Gritz,¹ C. Fumeaux,² and G. D. Boreman¹

¹School of Optics/CREOL
University of Central Florida
4000 Central Florida Boulevard
Orlando, Florida 32816-2700

²Swiss Federal Institute of Technology, ETH-Zurich
Laboratory for Electromagnetic Fields and Microwave Electronics
CH-8092 Zürich

Received February 21, 2002

Abstract

Antenna-coupled microbolometers are known for having short time constants and high responsivity, but their small dimensions make them unsuitable for imaging applications where a typical pixel area is generally greater than $20 \times 20 \mu\text{m}^2$. In this paper a two dimensional array of antenna-coupled microbolometers is demonstrated as an area receiver. Using the response of microbolometers to visible frequencies a two-dimensional diagnostic scan in the visible was performed on these arrays which allowed measurement of their homogeneity. Frequency response measurements gave time constants around 130 nsec, similar to the ones obtained for single element microbolometers which indicates that a detector of virtually any size can be fabricated without sacrificing time response. Response and noise measurements show lower noise and higher responsivity compared to single element microbolometers. These results make two-dimensional arrays of antenna-coupled microbolometers a promising option for development of pixels in infrared focal plane arrays.

Keywords: Microbolometer; antenna-coupled detector; infrared focal plane array.

1. Introduction

A bolometer is a resistive element made out of a material with large temperature coefficient of resistance (TCR) so that a large change in resistance will take place whenever the element absorbs infrared radiation. Bolometers are operated by supplying the resistive element with a bias current and measuring the resulting voltage.

With traditional bolometers the resistive element is not only used to detect radiation, but the surface is also used to collect radiation. The problem with this approach is that in order to collect a substantial amount of infrared radiation the resistive element needs to have a large capture cross section which translates into a large thermal mass which would yield in slow detectors.

By coupling an antenna to a small bolometer it is possible to have fast detectors without sacrificing collection area. The antenna will be the collection mechanism and the bolometer will detect the collected radiation. Also when the detector element is small (microbolometer), a small amount of energy will be needed to make a large change in resistance, therefore a smaller detector will have better responsivity.

These microbolometers can be as small as $1 \times 0.3 \mu\text{m}^2$ [1]. Detectors this small are unsuitable for imaging applications where a typical pixel area ranges from $20 \times 20 \mu\text{m}^2$ to $50 \times 50 \mu\text{m}^2$ [2]. In this paper a two-dimensional array of microbolometers is proposed to increase the area of the detector without sacrificing the high response and short time constant characteristic of microbolometers.

2. Structures and Fabrication

In order to keep the Johnson noise low a series-parallel combination of microbolometers, that will make the two-dimensional array have the same resistance as a single microbolometer, was fabricated. Figure 1 shows an electron microscope photograph of a 5×5 array of microbolometers that covers an area of $25 \times 25 \mu\text{m}^2$. The elements of the array are spaced $5 \mu\text{m}$ apart of each other in the x and y directions. The entire structure is defined using electron-beam lithography [1]. The arms of the dipole antenna, the bus bars (which connect in parallel the elements of the array), and the bond pads are made out of gold deposited using e-beam evaporation. The length of the individual dipole elements

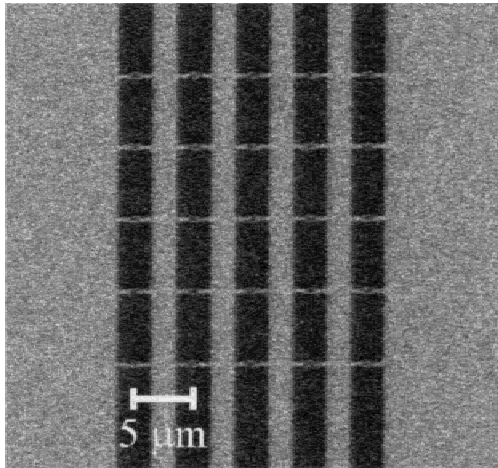


Figure 1. Scanning electron micrograph of a 5×5 array of microbolometers.

is $3 \mu\text{m}$, the bus bars are $2 \mu\text{m}$ wide and the arms of the dipole are approximately 200 nm wide. The thickness of the gold layer is 100 nm . The sensing element is a $0.8 \mu\text{m} \times 0.3 \mu\text{m}$ and 70 nm Nb patch deposited by sputtering.

Two types of arrays were fabricated, a 5×5 array and a 10×10 array. These devices were fabricated on high resistivity ($\rho \approx 3 \text{ k}\Omega \text{ cm}$) Si wafers coated with 150 nm of SiO_2 for thermal and electrical isolation. The wafers were scribed into 1 cm^2 chips and wire bonded to specially made chip carriers. Each chip contained 9 arrays and a single element microbolometer as test structure for performance comparisons.

The fabricated devices had a dc resistance of $155 \pm 2.6 \Omega$ for the single element structures, $292 \pm 9.5 \Omega$ for the 5×5 arrays, and $253 \pm 4.7 \Omega$ for the 10×10 arrays.

3. Experimental Method

Response measurements were made on single element bolometers, 5×5 arrays, and 10×10 arrays using a CO_2 -laser at $10.6 \mu\text{m}$. The laser beam was focused by an F/8 optical train to provide uniform irradiance over the largest receiving area ($50 \times 50 \mu\text{m}^2$ on the 10×10 array). The

resulting almost diffraction-limited spot had a $1/e^2$ radius of 200 μm and an irradiance of 360 W/cm^2 at the focus.

The chip containing the arrays, along with the amplifying circuit, was mounted on a three-axis positioning stage. The z direction (along the beam axis) was moved manually using a micrometer and the x and y axes were motorized by a Melles Griot NanomoverTM system with bidirectional repeatability of 100 nm. The motorized stage was controlled by a computer which was also in charge of the acquisition and storage of data. This positioning stage also had a rotational stage that would allow response as a function of angle of incidence (radiation pattern) measurements.

The microbolometers under test were biased so that each individual element received 200 μA of bias current. The devices under test were placed at the focus of the laser beam which was modulated with a chopper at a frequency of 2.5 kHz. The modulated signal produced by the device was read with a lock-in amplifier after a 10 \times amplification stage.

Noise measurements were made using an HP3585B spectrum analyzer. The root-mean-square (RMS) noise was obtained by integrating the frequency spectrum squared centered at 4 kHz and 12 kHz over a 2 kHz bandwidth, dividing it by the bandwidth and taking the square root.

Another optical train, using a HeNe laser at 632.8 nm and F/4 optics, was also used. This optical train presented a focal spot of 3 μm in radius. Response of antenna-coupled devices in the visible has been demonstrated before [3] therefore the use of an optical train in the visible will allow us to make high resolution measurements and test individual elements of the array.

4. Results

4.1. Measurements in the visible.

A two dimensional scan in the visible was performed on the arrays to verify the uniformity of its individual elements. The beam of the HeNe laser was focused in the center of the array by moving the detector along the three axes and maximizing its response. The two-dimensional scan was performed by keeping the z axis fixed, moving the device in the

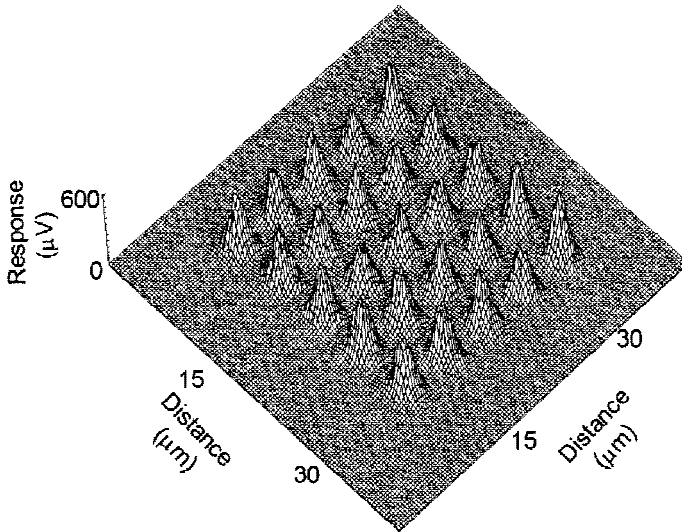


Figure 2. Two-dimensional scan in the visible for a 5×5 array of microbolometers.

x and y directions and recording the response of the device in each position. The length of the scan depended on the size of the arrays. For the 5×5 arrays a $40 \mu\text{m} \times 40 \mu\text{m}$ scan was performed and an $80 \mu\text{m} \times 80 \mu\text{m}$ scan was done for the 10×10 arrays, all of them using $0.3 \mu\text{m}$ steps in the x and y directions. Figure 2 shows a two-dimensional scan of a 5×5 array of microbolometers, on the scan the individual response of each element of the array can be observed. From the scan we can see how homogeneous are the microbolometers that form the array, this type of measurement can be used as a diagnostic tool to determine the quality of the array and detect possible defects in the fabrication process.

4.2. Detection Area.

A two-dimensional scan in the infrared was performed on a single element, 5×5 array and 10×10 array of microbolometers to determine the detection area covered by each device. The two-dimensional scans were taken following the same procedure used in section 4.1, but using a CO_2 laser at $10.6 \mu\text{m}$ and $F/1$ optics. The $F/1$ optics presented an almost

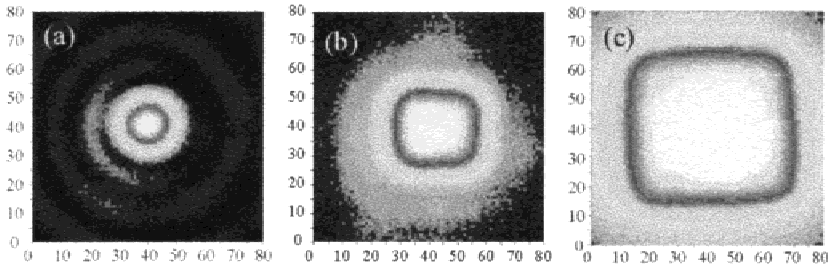


Figure 3. Two-dimensional scan in the infrared (CO₂ laser at 10.6 μm), for (a) Single Element, (b) 5 \times 5 array and (c) 10 \times 10 array of microbolometers. The dimensions are given in micrometers.

diffraction-limited focal spot of 12 μm in radius. Figures 3(a), 3(b) and 3(c) show 80 \times 80 μm^2 scans on a single element, 5 \times 5 array and 10 \times 10 array respectively. The scan on the single element (Figure 3(a)) showed only the beam profile, which indicates that the single element microbolometer can be considered as a point receiver at infrared frequencies. Figures 3(b) and 3(c) show how the detection area increases by going from a single element to a two-dimensional array of microbolometers. A uniform detection area of approximately 25 \times 25 μm^2 and 50 \times 50 μm^2 are shown in Figures 3(b) and 3(c) respectively, these areas correspond to the physical size of the receivers. From the results shown in Figure 3 we can see that two-dimensional arrays of microbolometers make uniform area detectors and can be used as pixel elements in infrared imaging systems.

4.3. Frequency Response.

The response of the two-dimensional arrays of microbolometers as a function of frequency was measured by taking out the chopper in the optical train and substituting it with an acousto-optic modulator. The laser beam was modulated in a range of frequencies that went from 0 Hz to 10 MHz. The time constant obtained for both 5 \times 5 and 10 \times 10 arrays was around 130 nsec, which is consistent with values obtained in the past for single element microbolometers [4]. These measurements indicate that we can construct a detector of any size without sacrificing time response.

4.4. Noise.

The two major sources of bolometer noise are Johnson noise and low-frequency ($1/f$) noise. The Johnson voltage noise, which is due to random motion of free carriers in any resistive material, is given by [5]

$$V_{n,J} = \sqrt{4KTR_b\Delta f} , \quad (1)$$

where K is Boltzmann's constant, T and R_b are the temperature and the resistance of the bolometer and Δf is the bandwidth of the measurement.

The $1/f$ voltage noise appears to result from imperfections in the resistor material structure and electrical contacts and, at frequency f , is given by [6]

$$V_{n,1/f} = V_b \sqrt{\frac{k\Delta f}{f}} , \quad (2)$$

where V_b is the voltage applied to the bolometer and k is a parameter that is dependent on the particular resistor (material, deposition technique, dimensions, electrical contacts, etc.)

The total noise of the bolometer V_n is the rms of the two noise components:

$$V_n = \sqrt{V_{n,J}^2 + V_{n,1/f}^2} . \quad (3)$$

From Eq. (3) we can see how at lower frequencies the $1/f$ noise component dominates and the noise of the bolometer increases, and at higher frequencies it becomes equal to the Johnson noise.

The series-parallel combination of microbolometers yield similar resistance values for different sizes of arrays. From Eq. (1) we can see that similar resistance values will give similar Johnson noise contributions. On the other hand the bias voltage applied to the arrays is 5 and 10 times higher than the one used to bias a single element

bolometer, therefore according to Eq. (2) the $1/f$ noise contribution should increase with the size of the array for equivalent biasing currents.

Noise measurements were made for the single element, 5×5 and 10×10 array, the results are shown in Figure 4. Surprisingly the noise level decreases with the number of elements in the array. Measurement of the noise as a function of bias voltage (Figure 5) shows that the noise dependence also decreases with higher number of elements in the array. From Eqs. (1)-(2) we can see that $1/f$ noise depends on the bias voltage therefore, contrary to what we expected, the $1/f$ noise contribution decreased with the number of elements in the array.

In order to take a closer look at the behavior of $1/f$ noise in these devices, measurements of noise versus frequency were made. Measurements made on a single element microbolometer (Figure 6) show the expected $1/f$ noise dependence. Measurements made on the arrays (Figure 7) show noise suppression at frequencies lower than 20 kHz, after 20 kHz the characteristic $1/f$ noise dependence appears again. This low-frequency noise reduction is due to the bus bars acting as guard structures and reducing the noise coupled through the substrate from each individual elements of the array to each other. Guard bands have been proven to reduce substantially low-frequency noise that propagates through the substrate [7].

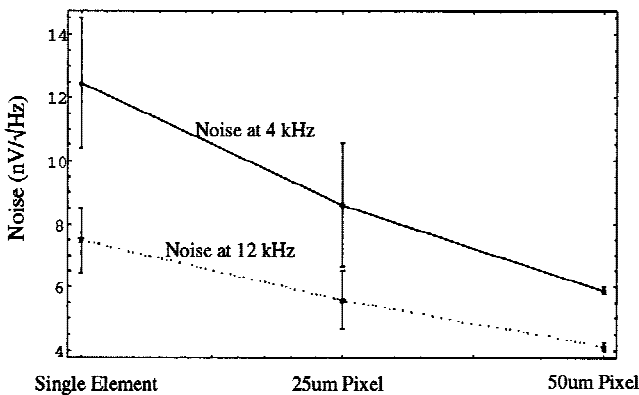


Figure 4. Noise measured for single element, 5×5 (25 μ m pixel) and 10×10 (50 μ m pixel) arrays.

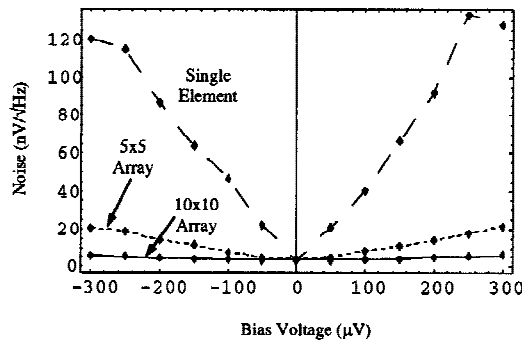


Figure 5. Noise as a function of bias voltage for single element, 5×5 and 10×10 arrays.

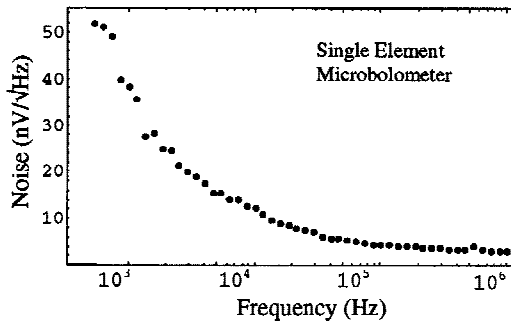


Figure 6. Noise as a function of frequency for a single element microbolometer.

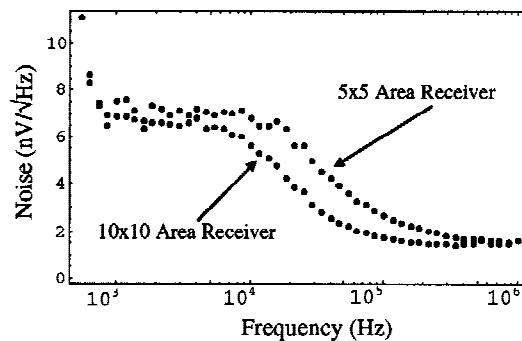


Figure 7. Noise as a function of frequency for a 5×5 and a 10×10 array of microbolometers.

4.5. Response.

The responsivity (in Volts/Watt) at low frequencies of a bolometer is given by [8]

$$\mathfrak{R} = \frac{i_{bias} R_b \alpha}{G_e}, \quad (4)$$

where i_{bias} is the bias current, R_b is the resistance of the bolometer, α is the temperature coefficient of resistance of the bolometer and G_e is the effective thermal conductance.

By putting N number of bolometers in series and applying the same bias current the response will go up by a factor of N due to the electrical addition of voltages. Figure 8 shows the response measured for a single element microbolometer, a 5×5 array and a 10×10 array. From Figure 8 we can see that going from a single element to a 5×5 array we get a factor of 5 increase in response, going to a 10×10 array we gain a factor of 8, close to the 5 and 10 times increase expected.

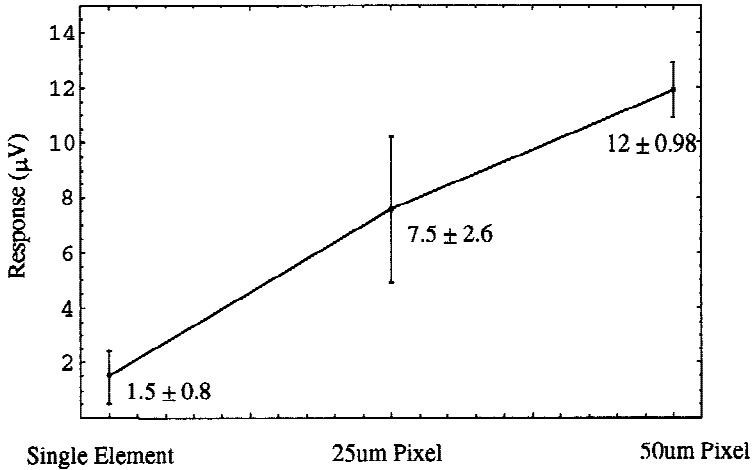


Figure 8. Response measurements for a single element, 5×5 (25μm pixel) and 10×10 (50μm pixel) arrays.

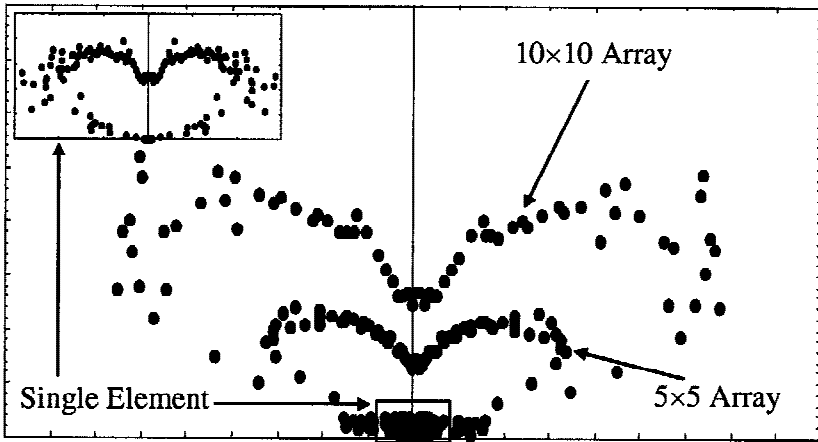


Figure 9. E-plane antenna patterns for a single element, 5×5 ($25\mu\text{m}$ pixel) and 10×10 ($50\mu\text{m}$ pixel) arrays of microbolometers.

Figure 9 shows the E-plane antenna patterns of a single element, 5×5 array and a 10×10 array of microbolometers, the antenna patterns are very similar which indicates that there is no significant electromagnetic coupling between the elements. To further increase the gain and directivity of the array two parameters need to be optimized, the length of the single element dipole, and the spacing between the elements. A length study on single element dipoles was performed by Fumeaux et al., finding the highest resonance at a length close to $1.2 \mu\text{m}$ [1]. The spacing of the elements has to be decreased to get better coupling between the elements and gain in responsivity through the antenna-array effect. A spacing of less than half the wavelength in the substrate (apparent wavelength) will avoid formation of grating lobes and the corresponding loss in power for normally incident radiation [9]. A spacing of about half the apparent wavelength will give more directive patterns, while putting the elements closer than half the apparent wavelength will yield an antenna pattern that resembles more the one of a single element. The apparent wavelength in the substrate was also investigated in [1] and was found to be $2.5 \mu\text{m}$ for $10.6 \mu\text{m}$ incident radiation.

5. Conclusions

Two-dimensional arrays of microbolometers that can cover the area of a picture element in an infrared imaging system have been fabricated and tested. These arrays can cover any area without sacrificing time response, which is very low for microbolometers. Taking advantage of their response to visible frequencies, a two-dimensional scan in the visible was performed on the two dimensional arrays of microbolometers. These measurements proved to be an effective way of characterizing the homogeneity of the detectors and the effectiveness of the fabrication process.

The influence of the array topology plays an important role in the performance of the arrays, the inclusion of wide bus bars to connect each microbolometer in parallel proved to be a low-frequency noise suppression mechanism that reduced the $1/f$ noise when going from single element microbolometers to arrays. This noise reduction will increase even more the signal-to-noise ratio of the arrays compared to single element microbolometers.

An increase in response was measured on two-dimensional arrays compared to single element microbolometers, an additional increase in response can be obtained by adjusting the distance between elements to get electromagnetic coupling which will allow vector addition of the collected radiation by the individual antenna elements (antenna array effect).

Aknowledgements

This material is based upon research supported by NASA grant NAG5-10308.

REFERENCES

1. C. Fumeaux, M. A. Gritz, I. Codreanu, W. L. Schaich, F. J. González, G. D. Boreman, "Measurement of the resonant lengths of infrared dipole antennas", *Infrared Physics & Technology*, 41 (2000), pp. 271-281.
2. Bajaj, J., "HgCdTe infrared detectors and focal plane arrays ", Conference on Optoelectronic and Microelectronic Materials Devices, 1998, pp. 23 -31.

3. C. Fumeaux, J. Alda, G. D. Boreman, "Lithographic antennas at visible frequencies", *Optics Letters*, 24 (22), 1999, pp. 1629-1631.
4. F. J. Gonzalez, C. Fumeaux, J. Alda, G. D. Boreman, "Thermal impedance model of electrostatic discharge effects on microbolometers", *Microwave and Optical Technology Letters*, 26 (5), 2000, pp. 291-293.
5. Sedky, S.; Fiorini, P.; Baert, K.; Hermans, L.; Mertens, R., "Characterization and optimization of infrared poly SiGe bolometers", *IEEE Transactions on Electron Devices*, 46 (4), 1999, pp. 675-682.
6. Kruse, P. W., Skatrud, D. D., *Uncooled Infrared Imaging Arrays and Systems*, Semiconductors and Semimetals vol. 47, Academic Press, 1997.
7. Nagata, M.; Nagai, J.; Hijikata, K.; Morie, T.; Iwata, A. , "Physical design guides for substrate noise reduction in CMOS digital circuits", *IEEE Journal of Solid-State Circuits*, 36 (3), 2001, pp. 539-549.
8. Richards, P. L., "Bolometers for infrared and millimeter waves", *J. Appl. Phys.* 76 (1), 1994, pp. 1-24.
9. Balanis, C. A., *Antenna Theory*, Second Edition, John Wiley, 1997.